

AlphaNet: Improved Training of Supernet with Alpha-Divergence

Dilin Wang¹ Chengyue Gong^{* 2} Meng Li^{* 1} Qiang Liu² Vikas Chandra¹

Abstract

Weight-sharing neural architecture search (NAS) is an effective technique for automating efficient neural architecture design. Weight-sharing NAS builds a supernet that assembles all the architectures as its sub-networks and jointly trains the supernet with the sub-networks. The success of weight-sharing NAS heavily relies on distilling the knowledge of the supernet to the sub-networks. However, we find that the widely used distillation divergence, i.e., KL divergence, may lead to student sub-networks that over-estimate or under-estimate the uncertainty of the teacher supernet, leading to inferior performance of the sub-networks. In this work, we propose to improve the supernet training with a more generalized α -divergence. By adaptively selecting the α -divergence, we simultaneously prevent the over-estimation or under-estimation of the uncertainty of the teacher model. We apply the proposed α -divergence based supernet training to both slimmable neural networks and weight-sharing NAS, and demonstrate significant improvements. Specifically, our discovered model family, AlphaNet, outperforms prior-art models on a wide range of FLOPs regimes, including BigNAS, Once-for-All networks, FBNetV3, and AttentiveNAS. We achieve ImageNet top-1 accuracy of 80.0% with only 444 MFLOPs.

1. Introduction

Designing accurate and computationally efficient neural network architectures is an important but challenging task. Neural architecture search (NAS) automates the neural network design by exploring an enormous architecture space and achieves state-of-the-art (SOTA) performance on various applications including image classification (Zoph & Le, 2017; Zoph et al., 2018), object detection (Ghiasi et al.,

^{*}Equal contribution ¹Facebook ²Department of Computer Science, The University of Texas at Austin. Correspondence to: Dilin Wang <wdilin@fb.com>.

2019), semantic segmentation (Zhang et al., 2019) and natural language processing (Wang et al., 2020b).

Conventional NAS approaches can be prohibitively expensive as hundreds of candidate architectures need to be trained from scratch and evaluated (e.g., Tan et al., 2019; Zoph et al., 2018). Supernet based approach has recently emerged to be a promising approach for efficient NAS. A supernet assembles all candidate architectures into a weight sharing network with each architecture corresponding to one sub-network. By training the sub-networks simultaneously with the supernet, different architectures can directly inherit the weights from the supernet for evaluation and deployment, which eliminates the huge cost of training or fine-tuning each architecture individually.

Though promising, supernet training is highly challenging in order to ensure that all the sub-networks are well trained (e.g., Yu et al., 2020; Cai et al., 2019a; Wang et al., 2020a). To stabilize the supernet training and improve the performance of sub-networks, one widely used approach is in-place knowledge distillation (KD) (Yu & Huang, 2019). Inplace KD leverages the soft labels predicted by the largest architecture in the supernet to supervise all the other sub-networks. By distilling the knowledge of the teacher model, the performance of the sub-networks can be improved significantly (Yu & Huang, 2019; Yu et al., 2020).

Standard knowledge distillation uses KL divergence to measure the discrepancy between the teacher and student networks. However, KL divergence penalizes the student model much more when it fails to cover one or more local modes of the teacher model (Murphy, 2012). Hence, the student model tends to over-estimate the uncertainty of the teacher model and suffers from inaccurate approximation of the most important mode, i.e., the correct prediction of the teacher model.

To further enhance the supernet training, we propose to replace the KL divergence with a more generalized α -divergence (Amari, 1985; Minka et al., 2005). Specifically, we show that by adaptively controlling α in the proposed divergence metric, we can penalize both the under-estimation and over-estimation of the teacher model uncertainty to encourage a more accurate approximation for the student models. While directly optimizing the proposed

adaptive α -divergence may suffer from a high variance of the gradients, we further propose a simple technique to clip the gradients of our adaptive α -divergence to stabilize the training process. We show the clipped gradients still define a valid divergence metric implicitly and hence, yielding a proper optimization objective for KD.

We empirically verify the proposed adaptive α -divergence in two notable applications of supernet - slimmable networks (Yu & Huang, 2019; Yu et al., 2018) and weight-sharing NAS (Yu et al., 2020; Wang et al., 2020a) on ImageNet. For weight-sharing NAS, we train a supernet containing both small (200M FLOPs) and large (2G FLOPs) sub-networks following Wang et al. (2020a). With the proposed adaptive α -divergence, we are able to train high-quality sub-networks, called AlphaNet, that surpass all prior state-of-the-art models in the range of 200 to 800 MFLOPs, like EfficientNets (Tan & Le, 2019), OFANets (Cai et al., 2019a), FBNetV3 (Dai et al., 2020), and BigNas (Yu et al., 2020). Specifically, AlphaNet-A4 achieves 80.0% accuracy with only 444 MFLOPs.

2. Background

Training high-quality supernet is fundamental for weight-sharing NAS but non-trivial (Benyahia et al., 2019). Recently, in-place KD is shown to be an effective mechanism that significantly improves the supernet performance (Yu & Huang, 2019; Yu et al., 2020).

To formalize the supernet training and in-place KD, consider a supernet with trainable parameter θ . Let \mathcal{A} denote the collection of all sub-networks contained in the supernet. The goal of training a supernet is to learn θ such that all the sub-networks in \mathcal{A} can be optimized simultaneously to achieve good accuracy.

The supernet training process with the in-place KD is illustrated in Figure 1. At each training step, given a mini-batch of data, the supernet as well as several sub-networks are sampled. While the supernet is trained with the real labels, all the sampled sub-networks are supervised with the soft labels predicted by the supernet. Then, the gradients from all the sampled networks are aggregated before the supernet parameters are updated. More formally, at the training step t , the supernet parameters θ are updated by

$$\theta_t \leftarrow \theta_{t-1} + \epsilon g(\theta_{t-1}),$$

where ϵ is the step size, and

$$g(\theta_{t-1}) = \nabla_{\theta} \left(\mathcal{L}_{\mathcal{D}}(\theta) + \gamma \mathbb{E}_s \mathcal{L}_{\text{KD}}([\theta, s]; \theta_{t-1}) \right) \Big|_{\theta=\theta_{t-1}}. \quad (1)$$

Here, $\mathcal{L}_{\mathcal{D}}(\theta)$ is the standard cross entropy loss of the supernet on a training dataset \mathcal{D} , γ is the weight coefficient,

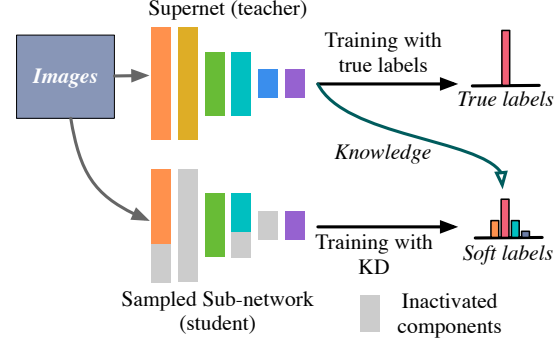


Figure 1. An illustration of training supernet with KD. Sub-networks are part of the supernet with weight-sharing.

and $\mathcal{L}_{\text{KD}}([\theta, s]; \theta_t)$ is the KD loss for distilling the supernet into a randomly sampled sub-network s , for which KL divergence has been widely used (e.g., Yu et al., 2020).

Let $p(x; \theta)$ and $q(x; \theta, s)$ denote the output probability of the supernet and the sub-network s given input x , then, we have

$$\mathcal{L}_{\text{KD}}([\theta, s], \theta_t) = \mathbb{E}_{x \sim \mathcal{D}} [\text{KL}(p(x; \theta_t) \parallel q(x; \theta, s))], \quad (2)$$

where $\text{KL}(p \parallel q) = \mathbb{E}_p [\log(p/q)]$. Note that the gradient on $p(x; \theta_t)$ in the KD loss is stopped as (2) indicated. For notation simplicity, we denote p as our teacher model and q (or q_{θ}) as student models in the following.

Additionally, note that the way KD is used in supernet training is different from the standard settings such as Hinton et al. (e.g., 2015), where the teacher network is pre-trained and fixed.

3. Supernet training with α -divergence

In this section, we analyze the limitations of using KL divergence in KD and propose to replace KL divergence with a more generalized α -divergence. We study the impact of different choices of α in the proposed divergence metric and further propose an adaptive algorithm to select α during the supernet training. Meanwhile, we also show that while directly optimizing α -divergence is challenging due to large gradient variances, a simple clipping strategy on α -divergence can be very effective to stabilize the training.

3.1. Classic KL based KD and its limitations

KL divergence has been widely used to measure the discrepancy in output probabilities between the teacher and student models in KD. One main drawback with KL divergence is that it cannot sufficiently penalize the student model when it over-estimates the uncertainty of the teacher model. Let p and q denote the output probability of the

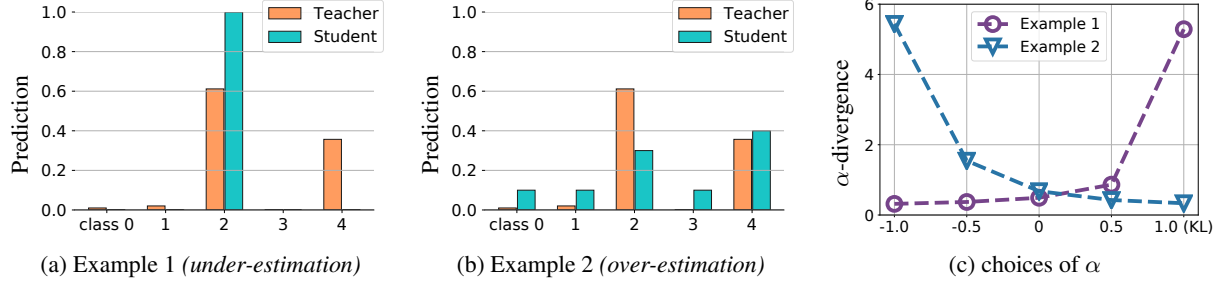


Figure 2. (a) *Example 1 - uncertainty under-estimation*. The student network under-estimates the uncertainty of the teacher model and misses important local modes of the teacher model. (b) *Example 2 - Uncertainty over-estimation*. In this case, the student network over-estimates the uncertainty of the teacher model and mis-classify the most dominant mode of the teacher model. (c) plots the corresponding α -divergences between the student model and the teacher model for *Examples 1* and *2*. Note that $\alpha = 1$ is a special case of KL divergence.

teacher and student models, respectively. The KL divergence between the teacher and student models is calculated by $\text{KL}(p||q) = \mathbb{E}_p[\log p/q]$. When $p > 0$, to ensure $\text{KL}(p||q)$ remains finite, we must have $q > 0$. This is the *zero avoiding* property of KL. In contrast, when $p = 0$, $q > 0$ does not get penalized. For example, as shown in Figure 2 (b) and (c), even though the student model over-estimates the uncertainty of the teacher model and predicts the wrong class ("class 4"), the KL divergence is still small.

The aforementioned *over-estimation* in Example 2 would be penalized at a larger magnitude when using other types of divergences, e.g., reverse KL divergence $\text{KL}(q||p)$. For reverse KL divergence, $\text{KL}(q||p) = \mathbb{E}_q[\log q/p]$ is infinite if $p = 0$ and $q > 0$. Hence if $p = 0$ we must ensure $q = 0$, this is known as the *zero forcing* property (Murphy, 2012). Therefore, minimizing reverse KL divergence encourages the student model q to avoid low probability modes of p while focusing on the modes with high probabilities, and thus, may *under-estimate* the uncertainty of the teacher model, as shown in Example 1 in Figure 2.

Hence, a natural question is whether it is possible to generalize the KL divergence to simultaneously suppress both the under-estimation and over-estimation of the teacher model uncertainty during the supernet training.

3.2. KD with adaptive α -divergence

Our observations shown in Figure 2 motivate us to design a new KD objective that simultaneously penalize both over-estimation and under-estimation of the teacher model uncertainty. We first generalize the typical KL divergence with a more flexible α -divergence (Minka et al., 2005). Consider $\alpha \in \mathbb{R} \setminus \{0, 1\}$, the α -divergence is defined as

$$D_\alpha(p||q) = \frac{1}{\alpha(\alpha-1)} \sum_{i=1}^m q_i \left[\left(\frac{p_i}{q_i} \right)^\alpha - 1 \right], \quad (3)$$

where $q = [q_i]_{i=1}^m$ and $p = [p_i]_{i=1}^m$ are two discrete distributions on m categories. The α -divergence includes a large spectrum of classic divergence measures. In particular, the KL divergence $\text{KL}(p||q)$ is the limit of $D_\alpha(p||q)$ with $\alpha \rightarrow 1$ while the reverse KL divergence $\text{KL}(q||p)$ is the limit of $D_\alpha(p||q)$ with $\alpha \rightarrow 0$.

A key feature of α -divergence is that we can decide to focus on penalizing different types of discrepancies (under-estimation or over-estimation) by choosing different α values. For example, as shown in Figure 2 (c), when α is negative, $D_\alpha(p||q)$ is large when q is more widely spread than p (when q *over-estimates* the uncertainty in p), and is small when q is more concentrated than p (when q *under-estimates* the uncertainty in p). The trend is opposite when α is positive: under-estimation would be more heavily penalized than over-estimation.

To simultaneously alleviate the over-estimation and under-estimation problem when training the supernet, we consider a positive α_+ and a negative α_- , and propose to use the maximum of $D_{\alpha_+}(p||q)$ and $D_{\alpha_-}(p||q)$ in the KD loss function:

$$D_{\alpha_+, \alpha_-}(p||q) = \max \left\{ \underbrace{D_{\alpha_-}(p||q)}_{\text{penalizing over-estimation}}, \underbrace{D_{\alpha_+}(p||q)}_{\text{penalizing under-estimation}} \right\}.$$

Our KL loss now changes from Eq (2) to

$$\mathcal{L}_{KD}([\theta, s], \theta_t) = \mathbb{E}_{x \sim \mathcal{D}} [D_{\alpha_+, \alpha_-}(p(x; \theta_t) || q(x; \theta, s))]. \quad (4)$$

We denote this KD strategy that always chooses the maximum of D_{α_-} and D_{α_+} to optimize as *Adaptive-KD*.

3.3. Stabilizing α -divergence KD

One would prefer to set both $|\alpha_+|$ and $|\alpha_-|$ to be large to ensure the student model is sufficiently penalized when it either under-estimates or over-estimates the uncertainty

the teacher model. However, directly optimizing the α -divergence with large $|\alpha|$ is often challenging in practice. Consider the gradient of α -divergence:

$$\nabla_{\theta} D_{\alpha}(p \parallel q_{\theta}) = -\frac{1}{\alpha} \mathbb{E}_{q_{\theta}} \left[\left(\frac{p}{q_{\theta}} \right)^{\alpha} \nabla_{\theta} \log q_{\theta} \right].$$

If $|\alpha|$ is large, then the powered term $(p/q_{\theta})^{\alpha}$ can be quite significant and cause the training process to be unstable. To enhance the training stability, we clamp the maximum value of $(p/q_{\theta})^{\alpha}$ to be β , and obtain

$$\tilde{\nabla}_{\theta} D_{\alpha}(p \parallel q_{\theta}) \stackrel{def}{=} -\frac{1}{\alpha} \mathbb{E}_{q_{\theta}} \left[\text{Clip}_{\beta} \left(\frac{p}{q_{\theta}} \right)^{\alpha} \nabla_{\theta} \log q_{\theta} \right], \quad (5)$$

where $\text{Clip}_{\beta}(t) = \min(t, \beta)$.

Eqn. (5) is a simple yet effective heuristic approximation of $\nabla_{\theta} D_{\alpha}(p \parallel q_{\theta})$. It is important to note that Eqn. (5) equals the *exact* gradient of a special f divergence between p and q_{θ} . Hence, our updates still amount to minimizing a valid divergence. Note that the clipping function $\text{Clip}_{\beta}(\cdot)$ is only partially differentiable. So naively clipping on $(p/q_{\theta})^{\alpha}$ in Eqn. (3) may stop gradients back-propagating from the density ratio terms, hence yielding gradients that are not from a valid divergence.

To show that we are still optimizing a valid divergence with Eqn. (5), note that, for a convex function $f: [0, +\infty) \rightarrow \mathbb{R}$, the f -divergence between p and q_{θ} is defined as

$$D_f(p \parallel q_{\theta}) = \mathbb{E}_{q_{\theta}} \left[f \left(\frac{p}{q_{\theta}} \right) - f(1) \right]. \quad (6)$$

Its gradient w.r.t. θ is

$$\nabla_{\theta} D_f(p \parallel q_{\theta}) = -\mathbb{E}_{q_{\theta}} \left[\rho_f \left(\frac{p}{q_{\theta}} \right) \nabla_{\theta} \log q_{\theta} \right],$$

where $\rho_f(t) = f'(t)t - f(t)$ (Wang et al. (2018)). Note that α -divergence is a special case of f -divergence when $f(t) = t^{\alpha}/(\alpha(\alpha-1))$.

Proposition 3.1. *There exists a convex function $f: (0, +\infty) \rightarrow \mathbb{R}$, such that $\tilde{\nabla}_{\theta} D_{\alpha}(p \parallel q_{\theta})$ in (5) is the exact gradient of $D_f(p \parallel q_{\theta})$, that is, $\tilde{\nabla}_{\theta} D_{\alpha}(p \parallel q_{\theta}) = \nabla_{\theta} D_f(p \parallel q_{\theta})$.*

Proof. Let $\rho_*(t) = \frac{1}{\alpha} \text{Clip}_{\beta}(t)^{\alpha}$. We just need to find an f such that

$$\rho_f(t) = f'(t)t - f(t) = \rho_*(t).$$

Taking derivation on both sides, we get $f''(t)t = \rho'_*(t)$. This gives $f''(t) = \rho'_*(t)/t$ and hence $f(t) = \int \int \rho'_*(t)/tdt$, where $\int \int$ denotes second-order antiderivative (or indefinite integral). Because $\rho_*(t)$ is non-decreasing, we have $\rho'_*(t)/t \geq 0$ for $t > 0$, and hence f is convex on $(0, +\infty)$. \square

Algorithm 1 Training supernet with α -divergence

- 1: **Input:** Adaptive α -divergence range given by α_- and α_+ , a clipping factor β , a supernet with parameter θ , search space \mathcal{A} .
- 2: **while** not converging **do**
- 3: Sample a mini-batch of data B .
- 4: Train the supernet with true labels from B
- 5: Draw k subnetworks $\{s_1, \dots, s_k\}$ from \mathcal{A} ; train sub-networks to mimic the supernet on the mini-batch data B with the KD loss defined in Eqn. (4) using clipped gradients in Eqn. (5).
- 6: **end while**

In practice, we apply equation (5) to the α -divergence used in equation (4). By clipping the value of importance weights, what we optimize is still a divergence metric but is more friendly to gradient-based optimization.

4. Experiments

We apply our Adaptive-KD to improve notable supernet-based applications, including slimmable neural networks (Yu & Huang, 2019) and weight-sharing NAS (e.g., Cai et al., 2019a; Yu et al., 2020; Wang et al., 2020a). We provide an overview of our algorithm for training supernet in Algorithm 1.

Adaptive-KD settings In our algorithm, α_- and α_+ control the magnitude of penalizing on *over-estimation* and *under-estimation*, respectively. And, β controls the range of density ratios between the teacher model and the student model. We find our method performs robustly w.r.t. a wide of range of choices of α_- , α_+ and β , yielding consistent improvements over the KL based KD baseline. Throughout the experimental section, we set $\alpha_- = -1$, $\alpha_+ = 1$ and $\beta = 5.0$ as default for our method. We provide detailed ablation studies on these hyper-parameters in section 4.4.

4.1. Slimmable Neural Networks

Slimmable neural networks (Yu et al., 2018; Yu & Huang, 2019) are examples of supernet that support a wide range of channel width configurations. The search space \mathcal{A} of slimmable networks contains networks with different width and all the other architecture configurations (e.g. depth, convolution type, kernel size) are the same. This way, slimmable networks allow different devices or applications to adaptively adjust the model width on the fly according to on-device resource constraints to achieve the optimal accuracy vs. energy efficiency trade-off.

Settings We closely follow the training recipe provided in Yu & Huang (2019), and use slimmable MobileNetV1

AlphaNet: Improved Training of Supernet with Alpha-Divergence

Model	Method	0.25×	0.3×	0.35×	0.4×	0.45×	0.5×	0.55×	0.6×	0.65×	0.7×	0.75×
MbV1	w/o KD	53.9	55.3	57.1	59.1	61.1	62.9	64.0	65.8	66.9	67.9	68.8
	w/ KL-KD	56.4	57.8	59.5	61.0	63.0	64.4	65.5	67.1	68.3	69.1	69.8
	w/ Adaptive-KD (ours)	56.4	57.9	59.7	61.7	63.4	65.0	66.2	67.7	68.8	69.5	70.1
MbV2	w/o KD	-	-	61.9	62.8	63.7	64.5	65.1	67.2	67.7	68.3	69.0
	w/ KL-KD	-	-	63.2	64.4	65.1	66.0	66.5	68.4	69.2	69.5	70.1
	w/ Adaptive-KD (ours)	-	-	63.7	64.6	65.6	66.3	66.9	68.7	69.3	69.9	70.5

Table 1. Top-1 validation accuracy on ImageNet for Slimmable MobileNetV1 networks (denoted by MbV1) and Slimmable MobileNetV2 networks (denoted by MbV2) trained with different KD strategies.

Model	Method	0.25×	0.3×	0.35×	0.4×	0.45×	0.5×	0.55×	0.6×	0.65×	0.7×	0.75×
MbV1	w/ KL-KD (T=0.5)	55.1	56.0	57.6	59.1	61.4	62.5	64.0	65.6	66.9	67.9	68.7
	T=2.0	55.4	57.0	58.8	60.7	62.6	64.1	65.3	66.6	67.9	68.7	69.5
	T=4.0	48.7	50.7	53.1	55.9	58.8	60.9	62.7	64.6	66.0	67.4	68.3
MbV2	w/ KL-KD (T=0.5)	-	-	61.7	62.9	63.8	64.6	65.0	67.4	68.4	68.8	69.8
	T=2.0	-	-	62.6	63.9	64.8	65.6	66.4	68.1	68.6	69.1	70.0
	T=4.0	-	-	59.3	60.9	62.2	63.1	64.0	66.3	67.1	67.7	68.8

Table 2. Comparison to KL based KD with different temperature (T) settings. We report top-1 validation accuracy on ImageNet for slimmable MobileNetV1 and MobileNetV2 networks, denoted by MbV1 and MbV2, respectively.

(Howard et al., 2017) and slimmable MobileNetV2 (Sandler et al., 2018) as our testbed. Specifically, we train slimmable MobileNetV1 to support arbitrary dynamic width in the range of $[0.25, 1.0]$, and train slimmable MobileNetV2 to support dynamic widths of $[0.35, 1.0]$.

We adopt the sandwich rule sampling proposed in Yu & Huang (2019) for training. At each training iteration, we sample the supernet with the largest channel width, the smallest sub-network with the smallest channel width and two random sub-networks to accumulate the gradients. We train the supernet with ground truth labels and train all subsampled sub-networks with KD following (1). For our baseline KD strategy, we set the KD coefficient γ to be the number of sub-networks sampled, i.e., $\gamma = 3$, as default following Yu & Huang (2019). To evaluate the effectiveness of our method, we simply replace the baseline KL-based KD loss used in Yu & Huang (2019) with our adaptive KD loss in (4).

Additionally, we train all models for 360 epochs using SGD optimizer with momentum as 0.9, weight decay as 10^{-5} and dropout as 0.2. We use cosine learning rate decay, with an initial learning rate of 0.8, and batch size of 2048 on 16 GPUs. Following Yu & Huang (2019), we evaluate on ImageNet (Deng et al., 2009). We note that the baseline models trained with our hyper-parameter settings outperform those reported in Yu & Huang (2019).

Results We summarize our results in Table 1. We report the top-1 accuracy on the ImageNet. Here, *w/o KD* denotes the training strategy that excludes the effect of KD. All such

sub-networks are trained with ground truth labels via cross entropy.

As we can see from Table 1, both baseline KL based KD (denoted as *w/ KL-KD*) and our adaptive KD (denoted as *w/ Adaptive-KD*) yield significant performance improvements compared to *w/o KD*. Our results confirm the importance of KD for training Slimmable networks. Meanwhile, our Adaptive-KD further improves on KL based KD for all the channel width configurations evaluated for both Slimmable MobileNetV1 (denoted by MbV1) and Slimmable MobileNetV2 (denoted by MbV2).

Comparison to KD with different temperature coefficients As discussed in Hinton et al. (2015), for standard KL based KD, one can soften (or sharpen) the probabilities of the teacher and the student model by applying a temperature in their softmax layers. The best distillation performance might be achieved with a different temperature other than the normally used temperature of 1.

To ensure a fair comparison, we further evaluate the baseline KL based KD under different temperature (T) settings following the approach in Hinton et al. (2015). We refer the reader to Appendix C for detailed discussion on this topic. In particular, we test a number of temperatures - 0.5, 2, 4. We summarize our results in Table 2. We find all these settings to systematically perform worse than the simple KD strategy without temperature scaling, i.e., $T = 1$. Additionally, the models trained via our method yield the best performance.

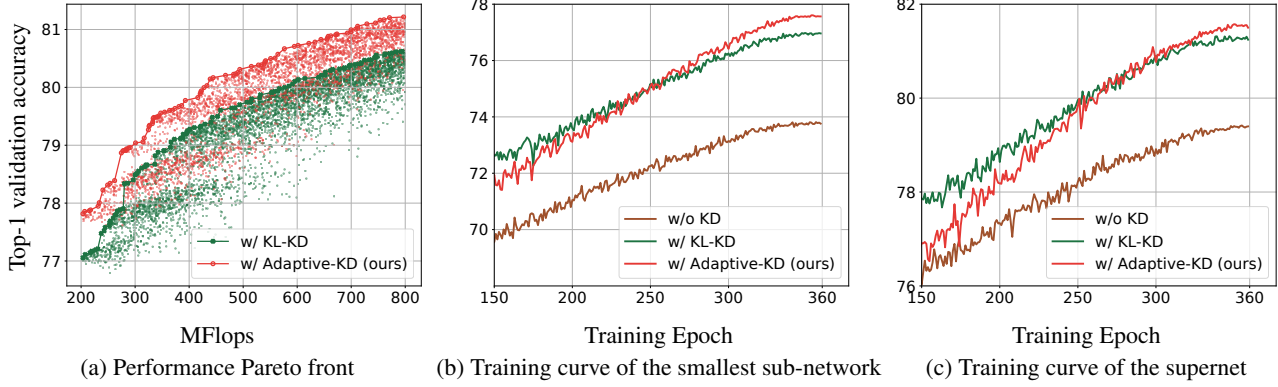


Figure 3. (a) Comparison of Pareto-set performance of the supernet trained via KL based KD and our adaptive KD, respectively. Each dot represents a sub-network evaluated during the evolutionary search step. (b-c) Training curves of the smallest sub-network and the largest sub-network (i.e., the supernet).

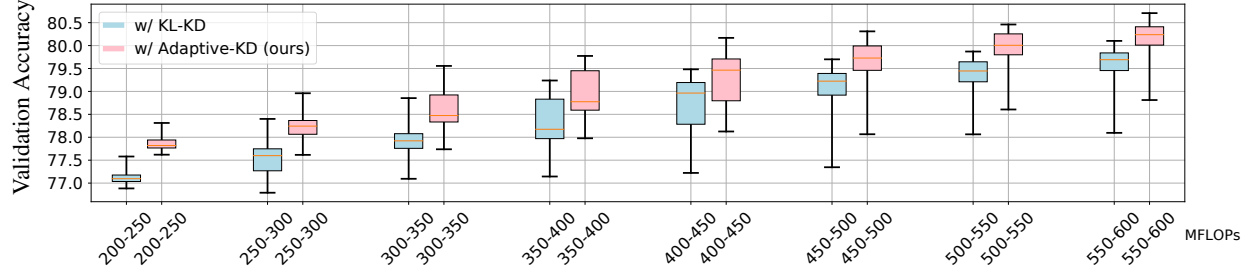


Figure 4. Top-1 accuracy on ImageNet from weight-sharing NAS with KL-based KD and adaptive-KD. Each box plot shows the performance of sampled sub-networks within each FLOPs regime. From bottom to top, each horizontal bar represents the minimum accuracy, the first quartile, the median, the third quartile and the maximum accuracy, respectively.

4.2. Weight-sharing NAS

We apply our Adaptive-KD to improve supernet for weight-sharing NAS (Cai et al., 2019a; Yu et al., 2020; Wang et al., 2020a). Please see Appendix A for a brief introduction on weight-sharing NAS. Note that one main procedure of weight-sharing NAS is to simultaneously train all sub-networks specified in the search space to converge. Similar to training Slimmable neural networks, this is often achieved by enforcing all sub-networks to learn from the supernet with KL based KD, (e.g., Yu et al., 2020).

Training. Our training recipe follows Wang et al. (2020a) except we use uniform sampling for simplicity. We pursue minimum code modifications to ablate the effectiveness of our KD strategy. We evaluate on the ImageNet dataset (Deng et al., 2009). All training details and the search space we used are discussed in Appendix B.

We use the update rule defined in (1) to train the supernet. Following Wang et al. (2020a) and Yu et al. (2020), at each iteration, we train the supernet with ground truth labels and simultaneously we train the smallest sub-network and two random sub-networks with KD. In this way, a total of 4

networks are trained at each iteration.

Evaluation We compare the accuracy vs. FLOPs Pareto formed by the supernet learned by different KD strategies. To estimate the performance Pareto, we proceed as follows: 1) we first randomly sample 512 sub-networks from the supernet and estimate their accuracy on the ImageNet validation set; 2) we apply crossover and random mutation on the best performing 128 sub-networks following Wang et al. (2020a). We fix both the crossover size and mutation size to be 128, yielding 256 new sub-networks. We then evaluate the performance of these sub-networks; 3) We repeat the second step 20 times. The total number of sub-networks thus evaluated is 5,376.

Results As we can see from Figure 3(a), *Adaptive-KD* achieves a significantly better Pareto frontier compared to the KL-based KD baseline (denoted as *w/ KL-KD*) and the simple training strategy without KD (denoted as *w/o KD*). Figures 3(b) and (c) plot the convergence curve of the smallest sub-network and the supernet, respectively. Our method adaptively optimizes a more difficult KD loss between the supernet and the sub-networks, yielding slightly

	A0 (203M)	A1(279M)	A2(317M)	A3(357M)	A4(444M)	A5 (491M)	A6 (709M)
w/o KD	73.8	75.4	75.6	76.0	76.8	77.1	77.9
w/ KL-KD	77.0	78.2	78.5	78.8	79.3	79.6	80.1
w/ KL-KD + Attentive Sampling [†]	77.3	78.4	78.8	79.1	79.8	80.1	80.7
w/ Adaptive-KD (ours - AlphaNet)	77.8	78.9	79.1	79.4	80.0	80.3	80.8

Table 3. Performance on the discovered networks in Wang et al. (2020a). Each (#M) denotes the MFLOPs of the corresponding model. [†] uses additional attentive sampling (Wang et al., 2020a) for training supernet. We denote our models as AlphaNet.

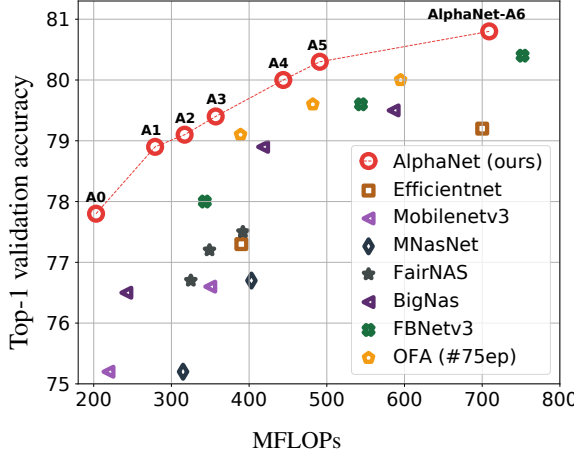


Figure 5. Comparison with prior art NAS approaches on ImageNet. #75ep denotes the models are further finetuned for 75 epochs with weights inherited from the corresponding supernet.

slower convergence in the early stage of the training but better performance towards the end of the training.

In Figure 4, we group sub-networks according to their FLOPs and visualize five statistics for each group of sub-networks, including the minimum, the first quantile, the median, the third quantile and the maximum accuracy. Our method learns significantly better sub-networks in a quantitative way.

Improvement on SOTA As we use the same search space as in Wang et al. (2020a), we further evaluate the discovered AttentiveNAS models (from A0 to A6) with the supernet weights learned by our adaptive KD. We call our models as AlphaNet.

As we can see from Table 3, our Adaptive-KD significantly improves on classic KL based KD, yielding an average of 0.7% improvements in the top-1 accuracy from A0 to A6. Also, our AlphaNet outperform all corresponding AttentiveNAS models (Wang et al., 2020a), which requires building Pareto-aware sampling distributions with additional computational overhead.

We further compare our AlphaNet against prior art NAS baselines, including EfficientNet (Tan & Le, 2019), FB-

Dataset	Eff-B0	Alp-A0	Eff-B1	Alp-A6
Oxford Flowers	97.2	97.7	97.8	98.7
Oxford-IIIT Pets	91.2	91.5	92.4	92.9
Food-101	87.6	88.3	89.0	89.6
Stanford Cars	91.0	91.5	92.2	92.6
FGVC Aircraft	88.1	88.5	88.7	89.1

Table 4. Comparison of transfer learning accuracy. ‘Eff’ and ‘Alp’ denotes EfficientNet and AlphaNet, respectively. All the networks are pretrained on ImageNet and then finetuned on transfer learning datasets. EfficientNet-B0 and B1 has a model size of 390 MFLOPs and 700 MFLOPs, respectively. AlphaNet-A0 and A6 use 203 MFLOPs and 709 MFLOPs, respectively.

NetV3 (Dai et al., 2020), BigNAS (Yu et al., 2020), OFA (Cai et al., 2019a), MobileNetV3 (Howard et al., 2019), FairNAS (Chu et al., 2019) and MNasNet (Tan et al., 2019), in Figure 5. Our method outperforms all the baselines evaluated, establishing new SOTA accuracy vs. FLOPs trade-offs on ImageNet. For example, our model achieves 77.8% top-1 accuracy with only 203 MFLOPs. Under similar FLOPs constraint, the corresponding top-1 accuracy is 75.2% with 219 MFLOPs for MobileNetV3, 76.5% top-1 accuracy with 242 MFLOPs for BigNAS. Compared to OFA, our model achieves the same 80.0% top-1 accuracy with 35% fewer FLOPs (444M v.s. 595M) and the same 79.1% top-1 accuracy with 26% fewer FLOPs (317M v.s. 400M).

4.3. Transfer learning

We take our AlphaNet-A0 and AlphaNet-A6 models that are pretrained on ImageNet and fine-tune them on a number of transfer learning benchmarks. We closely follow the training settings in EfficientNet (Tan & Le, 2019) and GPipe (Huang et al., 2018). Specifically, we use SGD with momentum of 0.9, label smoothing of 0.1 and dropout of 0.5. All models are fine-tuned for 150 epochs with batch size of 64. Following Huang et al. (2018), we search the best learning rate and weight decay on a hold-out subset (20%) of the training data.

Transfer learning results We evaluated on five transfer learning datasets, including Oxford Flowers (Nilsback & Zisserman, 2008), Oxford Pets (Parkhi et al., 2012), Food-

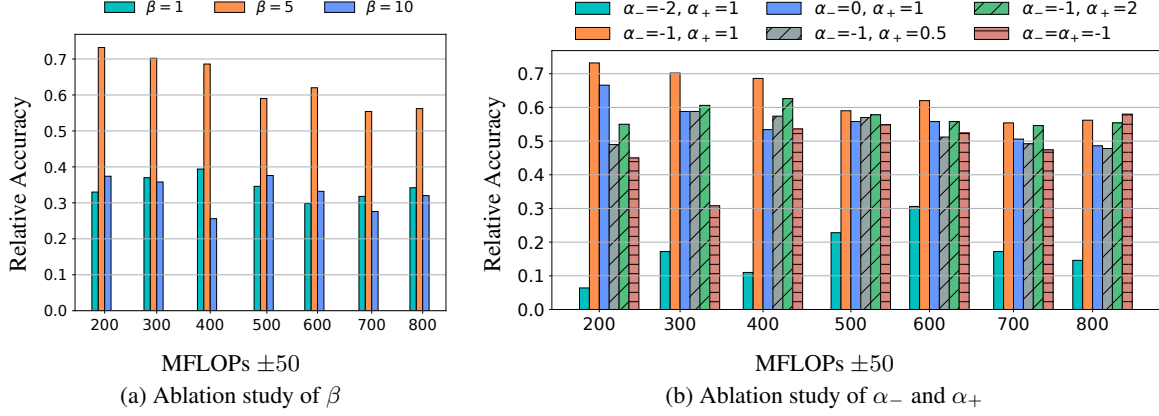


Figure 6. Relative accuracy compared to the results of KL based KD. Figure (a): we fix $\alpha_- = -1, \alpha_+ = 1$ and study the effect of our clipping factor β . Figure (b): we set $\beta = 5$ as default and study the impact of α_- and α_+ .

Model	w/o KD	w/ KL-KD (T=1)	T=2	T=4	Adaptive-KD
MobileNetV3 0.75 \times	73.3	73.9	72.2	70.8	73.9
MobileNetV3 0.5 \times	69.6	69.8	65.4	63.6	70.0

Table 5. Comparison to KL based KD with a fixed teacher model. Here T denotes the temperature used in classic KL based KD (see Appendix C). We use MobileNetV3 1.0 \times as our teacher model, which yields 75.4% top-1 validation accuracy on ImageNet.

101 (Bossard et al., 2014), Stanford Cars (Krause et al., 2013) and Aircraft (Maji et al., 2013). As we can see from Table 4, our AlphaNet-A0 and AlphaNet-A6 models lead to significant better transfer learning accuracy compared to those from EfficientNet-B0 and EfficientNet-B1 models.

4.4. Additional results

Robustness w.r.t. clipping factor β We follow the training and evaluation settings in section 4.2 and study the effect of β . In Figure 6 (a), we group sub-networks according to their FLOPs, and report the relative top-1 accuracy improvements of the maximum top-1 accuracy of each FLOPs group over the result from the KL based KD baseline. As shown in Figure 6(a), our algorithm is robust to the choice of β . Our algorithm works with a large range of β , from 1 to 10, yielding consistent improvements over the classic KL based KD baseline. And our default setting $\beta = 5$ achieves best performance on all FLOPs regimes evaluated.

Robustness w.r.t. α We ablate the impact of both α_- and α_+ under the same settings as in section 4.2. In this case, we fix $\beta = 5$. We present our findings in Figure 6(b). Firstly, we test with $\alpha_- = -2, -1, 0$, with α_+ fixed as 1. With a more negative α (e.g., $\alpha_- = -2$), this defines a more difficult objective that brings optimization challenges. With a large α_- (e.g., $\alpha_- = 0$), the resulting KD loss is less discriminative regarding uncertainty over-estimation. Overall, $\alpha_- = -1$ achieves a good balance between optimization difficulty and over-estimation penalization, yielding the best performance; Secondly, we vary

α_+ from 0.5 to 2, with α_- fixed as -1 . Similarly, we find that large α_+ (e.g., $\alpha_+ = 1$) yields the best performance; Lastly, we set both $\alpha_- = \alpha_+ = -1$. In this case, we still achieve better performance compared to the results of our KL based KD baseline, indicating the importance of penalizing over-estimation in training sub-networks. Also, our adaptive KD that regularizes on both over-estimation and under-estimation achieves better performance in general.

Improvement on single network training Additionally, we apply our Adaptive-KD to train a single neural network with a pretrained teacher model, as in convolutional KD setup (See Appendix C). Specifically, we use MobileNetV3 1.0 \times (Howard et al., 2019) as our teacher model and train MobileNetV3 0.5 \times and 0.75 \times as our student models. We summarize the top-1 validation accuracy on ImageNet from the models trained with different KD strategies in Table 5. The student models trained via our method yield the best accuracy.

5. Conclusion

In this work, we propose a method to improve the training of supernet with α -divergence based knowledge distillation. By adaptively selecting an α -divergence to optimize, our method simultaneously penalizes *over-estimation* and *under-estimation* in KD. Applying our method for neural architecture search, the searched AlphaNet models establish new state-of-the-art accuracy vs. FLOPs trade-offs on the ImageNet dataset.

References

Sungsoo Ahn, Shell Xu Hu, Andreas Damianou, Neil D Lawrence, and Zhenwen Dai. Variational information distillation for knowledge transfer. In *Proceedings of the IEEE/CVF Conference on Computer Vision and Pattern Recognition*, pp. 9163–9171, 2019.

Shun-ichi Amari. Differential-geometrical methods in statistics. *Lecture Notes on Statistics*, 28:1, 1985.

Yassine Benyahia, Kaicheng Yu, Kamil Bennani Smires, Martin Jaggi, Anthony C Davison, Mathieu Salzmann, and Claudiu Musat. Overcoming multi-model forgetting. In *International Conference on Machine Learning*, pp. 594–603. PMLR, 2019.

Lukas Bossard, Matthieu Guillaumin, and Luc Van Gool. Food-101-mining discriminative components with random forests. In *European conference on computer vision*, pp. 446–461. Springer, 2014.

Han Cai, Chuang Gan, Tianzhe Wang, Zhekai Zhang, and Song Han. Once-for-all: Train one network and specialize it for efficient deployment. In *International Conference on Learning Representations*, 2019a.

Han Cai, Ligeng Zhu, and Song Han. Proxylessnas: Direct neural architecture search on target task and hardware. *International Conference on Learning Representations*, 2019b.

Xiangxiang Chu, Bo Zhang, Ruijun Xu, and Jixiang Li. Fairnas: Rethinking evaluation fairness of weight sharing neural architecture search. *arXiv preprint arXiv:1907.01845*, 2019.

Ekin D Cubuk, Barret Zoph, Dandelion Mane, Vijay Vasudevan, and Quoc V Le. Autoaugment: Learning augmentation policies from data. *Proceedings of the IEEE/CVF Conference on Computer Vision and Pattern Recognition*, 2018.

Xiaoliang Dai, Alvin Wan, Peizhao Zhang, Bichen Wu, Zijian He, Zhen Wei, Kan Chen, Yuandong Tian, Matthew Yu, Peter Vajda, et al. Fbnetv3: Joint architecture-recipe search using neural acquisition function. *arXiv preprint arXiv:2006.02049*, 2020.

Jia Deng, Wei Dong, Richard Socher, Li-Jia Li, Kai Li, and Li Fei-Fei. Imagenet: A large-scale hierarchical image database. In *IEEE conference on computer vision and pattern recognition*, pp. 248–255. Ieee, 2009.

Golnaz Ghiasi, Tsung-Yi Lin, and Quoc V Le. Nas-fpn: Learning scalable feature pyramid architecture for object detection. In *Proceedings of the IEEE/CVF Conference on Computer Vision and Pattern Recognition*, pp. 7036–7045, 2019.

Geoffrey Hinton, Oriol Vinyals, and Jeff Dean. Distilling the knowledge in a neural network. *arXiv preprint arXiv:1503.02531*, 2015.

Andrew Howard, Mark Sandler, Grace Chu, Liang-Chieh Chen, Bo Chen, Mingxing Tan, Weijun Wang, Yukun Zhu, Ruoming Pang, Vijay Vasudevan, et al. Searching for mobilenetv3. In *Proceedings of the IEEE/CVF International Conference on Computer Vision*, pp. 1314–1324, 2019.

Andrew G Howard, Menglong Zhu, Bo Chen, Dmitry Kalenichenko, Weijun Wang, Tobias Weyand, Marco Andreetto, and Hartwig Adam. Mobilenets: Efficient convolutional neural networks for mobile vision applications. *arXiv preprint arXiv:1704.04861*, 2017.

Jie Hu, Li Shen, and Gang Sun. Squeeze-and-excitation networks. In *Proceedings of the IEEE conference on computer vision and pattern recognition*, pp. 7132–7141, 2018.

Yanping Huang, Youlong Cheng, Ankur Bapna, Orhan Firat, Mia Xu Chen, Dehao Chen, HyoukJoong Lee, Jiquan Ngiam, Quoc V Le, Yonghui Wu, et al. Gpipe: Efficient training of giant neural networks using pipeline parallelism. *Advances in Neural Information Processing Systems*, 2018.

Zehao Huang and Naiyan Wang. Like what you like: Knowledge distill via neuron selectivity transfer. *arXiv preprint arXiv:1707.01219*, 2017.

Yunhun Jang, Hankook Lee, Sung Ju Hwang, and Jinwoo Shin. Learning what and where to transfer. In *International Conference on Machine Learning*, pp. 3030–3039. PMLR, 2019.

Kirthevasan Kandasamy, Willie Neiswanger, Jeff Schneider, Barnabas Poczos, and Eric Xing. Neural architecture search with bayesian optimisation and optimal transport. *Advances in Neural Information Processing Systems*, 2018.

Jonathan Krause, Jia Deng, Michael Stark, and Li Fei-Fei. Collecting a large-scale dataset of fine-grained cars. *Second Workshop on Fine-Grained Visual Categorization*, 2013.

Zhuohan Li, Zi Lin, Di He, Fei Tian, Tao Qin, Liwei Wang, and Tie-Yan Liu. Hint-based training for non-autoregressive machine translation. *Empirical Methods in Natural Language Processing*, 2019.

Hanxiao Liu, Karen Simonyan, and Yiming Yang. Darts: Differentiable architecture search. *International Conference on Learning Representations*, 2019.

Subhransu Maji, Esa Rahtu, Juho Kannala, Matthew Blaschko, and Andrea Vedaldi. Fine-grained visual classification of aircraft. *arXiv preprint arXiv:1306.5151*, 2013.

Tom Minka et al. Divergence measures and message passing. Technical report, Citeseer, 2005.

Kevin P Murphy. *Machine learning: a probabilistic perspective*, chapter 21. MIT press, 2012.

Maria-Elena Nilsback and Andrew Zisserman. Automated flower classification over a large number of classes. In *2008 Sixth Indian Conference on Computer Vision, Graphics & Image Processing*, pp. 722–729. IEEE, 2008.

Wonpyo Park, Dongju Kim, Yan Lu, and Minsu Cho. Relational knowledge distillation. In *Proceedings of the IEEE/CVF Conference on Computer Vision and Pattern Recognition*, pp. 3967–3976, 2019.

Omkar M Parkhi, Andrea Vedaldi, Andrew Zisserman, and CV Jawahar. Cats and dogs. In *IEEE conference on computer vision and pattern recognition*, pp. 3498–3505. IEEE, 2012.

Nikolaos Passalis and Anastasios Tefas. Learning deep representations with probabilistic knowledge transfer. In *Proceedings of the European Conference on Computer Vision (ECCV)*, pp. 268–284, 2018.

Hieu Pham, Melody Guan, Barret Zoph, Quoc Le, and Jeff Dean. Efficient neural architecture search via parameters sharing. In *International Conference on Machine Learning*, pp. 4095–4104. PMLR, 2018.

Esteban Real, Alok Aggarwal, Yanping Huang, and Quoc V Le. Regularized evolution for image classifier architecture search. In *Proceedings of the aaai conference on artificial intelligence*, volume 33, pp. 4780–4789, 2019.

Adriana Romero, Nicolas Ballas, Samira Ebrahimi Kajou, Antoine Chassang, Carlo Gatta, and Yoshua Bengio. Fitnets: Hints for thin deep nets. *arXiv preprint arXiv:1412.6550*, 2014.

Mark Sandler, Andrew Howard, Menglong Zhu, Andrey Zhmoginov, and Liang-Chieh Chen. Mobilenetv2: Inverted residuals and linear bottlenecks. In *Proceedings of the IEEE conference on computer vision and pattern recognition*, pp. 4510–4520, 2018.

Mingxing Tan and Quoc Le. Efficientnet: Rethinking model scaling for convolutional neural networks. In *International Conference on Machine Learning*, pp. 6105–6114. PMLR, 2019.

Mingxing Tan, Bo Chen, Ruoming Pang, Vijay Vasudevan, Mark Sandler, Andrew Howard, and Quoc V Le. Mnasnet: Platform-aware neural architecture search for mobile. In *Proceedings of the IEEE/CVF Conference on Computer Vision and Pattern Recognition*, pp. 2820–2828, 2019.

Dilin Wang, Hao Liu, and Qiang Liu. Variational inference with tail-adaptive f-divergence. *arXiv preprint arXiv:1810.11943*, 2018.

Dilin Wang, Meng Li, Chengyue Gong, and Vikas Chandra. Attentivenas: Improving neural architecture search via attentive sampling. *arXiv preprint arXiv:2011.09011*, 2020a.

Hanrui Wang, Zhanghao Wu, Zhijian Liu, Han Cai, Ligeng Zhu, Chuang Gan, and Song Han. Hat: Hardware-aware transformers for efficient natural language processing. *arXiv preprint arXiv:2005.14187*, 2020b.

Junho Yim, Donggyu Joo, Jihoon Bae, and Junmo Kim. A gift from knowledge distillation: Fast optimization, network minimization and transfer learning. In *Proceedings of the IEEE Conference on Computer Vision and Pattern Recognition*, pp. 4133–4141, 2017.

Jiahui Yu and Thomas S Huang. Universally slimmable networks and improved training techniques. In *Proceedings of the IEEE International Conference on Computer Vision*, pp. 1803–1811, 2019.

Jiahui Yu, Linjie Yang, Ning Xu, Jianchao Yang, and Thomas Huang. Slimmable neural networks. *International Conference on Learning Representations*, 2018.

Jiahui Yu, Pengchong Jin, Hanxiao Liu, Gabriel Bender, Pieter-Jan Kindermans, Mingxing Tan, Thomas Huang, Xiaodan Song, Ruoming Pang, and Quoc Le. Bignas: Scaling up neural architecture search with big single-stage models. *European conference on computer vision*, 2020.

Yiheng Zhang, Zhaofan Qiu, Jingren Liu, Ting Yao, Dong Liu, and Tao Mei. Customizable architecture search for semantic segmentation. In *Proceedings of the IEEE/CVF Conference on Computer Vision and Pattern Recognition*, pp. 11641–11650, 2019.

Barret Zoph and Quoc V Le. Neural architecture search with reinforcement learning. *International Conference on Learning Representations*, 2017.

Barret Zoph, Vijay Vasudevan, Jonathon Shlens, and Quoc V Le. Learning transferable architectures for scalable image recognition. In *Proceedings of the IEEE conference on computer vision and pattern recognition*, pp. 8697–8710, 2018.

A. Weight-sharing NAS

Most RL-based NAS (e.g., Zoph & Le, 2017) and differentiable NAS (Liu et al., 2019; Cai et al., 2019b) consist of the following two stages as shown in Figure 7:

- 1) Stage 1 (architecture searching) - search potential architectures following a single resource constraint by using black-box optimization techniques (e.g., Zoph & Le, 2017) or differentiable weight-sharing based approaches (e.g., Liu et al., 2019; Cai et al., 2019b);
- 2) Stage 2 (retraining) - retrain deep neural networks (DNNs) found in step 1) from scratch for best accuracy and final deployment.

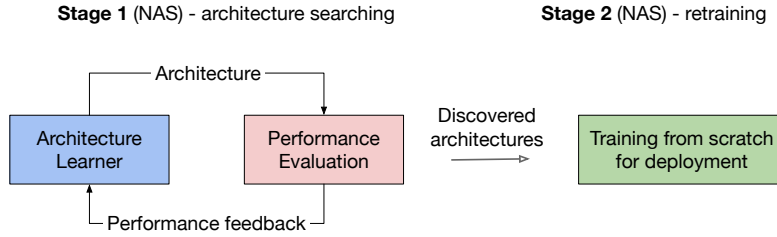


Figure 7. An overview of conventional NAS pipeline.

Though promising results have been demonstrated, these NAS methods usually suffer from the following disadvantages: 1) need to re-do the NAS search for different hardware resource constraints; 2) require training the selected candidate from scratch to achieve desirable accuracy; 3) especially for RL-based NAS that uses black-box optimization techniques, it requires training a large number of neural networks from scratch or on proxy tasks; These disadvantages significantly increase the computational cost of NAS and make the NAS search computationally expensive.

Supernet-based Weight-sharing NAS To alleviate the aforementioned issues, supernet-based weight-sharing NAS transforms the previous NAS training and search procedures as follows; see Figure 8.

- 1) Stage 1 (supernet pretraining): jointly optimize the supernet and all possible sub-networks specified in the search space, such that all searchable networks simultaneously achieve good performance at the end of the training phase.
- 2) Stage 2 (searching & deployment): After stage 1 training, all the sub-networks are optimized simultaneously. One could then use typical searching algorithms, like evolutionary algorithms, to search the best model of interest. The model weights of each sub-network are directly inherited from the pre-trained supernet without any further re-training or fine-tuning.

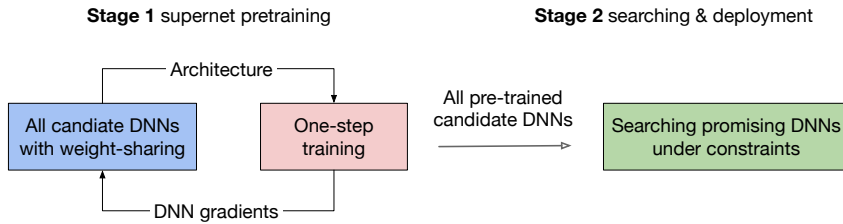


Figure 8. An overview of supernet-based weight-sharing NAS.

Compared to RL-based NAS and differentiable NAS algorithms, the key advantages of the supernet-based weight-sharing NAS pipeline are: 1) one needs to only perform the computationally expensive supernet training for once. All sub-networks defined in the search space are ready to use after stage 1 is fully optimized. No retraining or fine-tuning is required; 2) all sub-networks of various model sizes are jointly optimized in stage 1, finding a set of Pareto optimal models that naturally supports various resource considerations.

Notable examples of supernet-based weights-sharing NAS include BigNAS (Yu et al., 2020), OFA (Cai et al., 2019a), AttentiveNAS (Wang et al., 2020a) and HAT (Wang et al., 2020b).

B. Weights-sharing NAS training settings

We exactly follow the training settings in Wang et al. (2020a)¹. Specifically, we train our supernets for 360 epochs with cosine learning rate decay. We adopt SGD training on 64 GPUs. The mini-batch size is 32 per GPU. We use momentum of 0.9, weight decay of 10^{-5} , dropout of 0.2, stochastic layer dropout of 0.2. The base learning rate is set as 0.1 and is linearly scaled up for every 256 training samples. We use AutoAugment (Cubuk et al., 2018) for data augmentation and set label smoothing coefficient to 0.1.

We use the same search space provided in Wang et al. (2020a), see Table 6. Here Conv denotes regular convolutional layers and MBConv refers to inverted residual block proposed by Sandler et al. (2018). We use swish activation. Channel width represents the number of output channels of the block. MBPool denotes the efficient last stage in Howard et al. (2019). SE represents the squeeze and excite layer (Hu et al., 2018). *Input resolution* denotes the candidate resolutions. To simplify the data loading procedure, we always pre-fetch training patches of a fixed size, e.g., 224x224 on ImageNet, and then rescale them to our target resolution with bicubic interpolation following (Yu et al., 2020).

Block name	Channel width	Depth	Kernel size	Expansion ratio	SE
Conv	{16, 24}	-	3	-	-
MBConv-1	{16, 24}	{1,2}	{3, 5}	1	N
MBConv-2	{24, 32}	{3, 4, 5}	{3, 5}	{4, 5, 6}	N
MBConv-3	{32, 40}	{3, 4, 5, 6}	{3, 5}	{4, 5, 6}	Y
MBConv-4	{64, 72}	{3, 4, 5, 6}	{3, 5}	{4, 5, 6}	N
MBConv-5	{112, 128}	{3, 4, 5, 6, 7, 8}	{3, 5}	{4, 5, 6}	Y
MBConv-6	{192, 200, 208, 216}	{3, 4, 5, 6, 7, 8}	{3, 5}	6	Y
MBConv-7	{216, 224}	{1, 2}	{3, 5}	6	Y
MBPool	{1792, 1984}	-	1	6	-
Input resolution			{192, 224, 256, 288}		

Table 6. An illustration of our search space. Every row denotes a block group.

C. Knowledge distillation

Consider the image classification task over a set of classes $[m] := \{1, \dots, m\}$, where we have a collection of training images and one-hot labels $\mathcal{D}^{train} = \{(x, y)\}$ with $(x, y) \in \mathcal{X} \times \mathcal{Y}$ and $y \in \{0, 1\}^m$. We are interested in designing a deep neural network $q(x; \theta) : \mathcal{X} \rightarrow \mathcal{Y}$ that captures the relationship between x and y . Here θ is the network parameters of interest.

KD provides an effective way to train q by distilling knowledge from a teacher model in addition to the one-hot labels. The teacher network is often a relatively larger network with better performance. Specifically, let p be the teacher network, KD enforces q to mimic the output of p by minimizing the closeness between q and p , which is often specified by the KL divergence $D_{KL}(p \parallel q)$, yielding the following loss function,

$$\begin{aligned}
 \mathcal{L}(\theta) &= (1 - \beta)\mathcal{L}_{ERM}(\theta) + \beta\mathcal{L}_{KD}(\theta), \quad \text{with} \\
 \mathcal{L}_{ERM}(\theta) &= \mathbb{E}_{(x, y) \sim \mathcal{D}^{train}} \left[\mathcal{L}(y, q(x; \theta)) \right], \\
 \mathcal{L}_{KD}(\theta) &= \mathbb{E}_{x \sim \mathcal{D}^{train}} \left[D_{KL}(p(x) \parallel q(x; \theta)) \right]. \tag{7}
 \end{aligned}$$

Here $\mathcal{L}(\cdot)$ represents the empirical loss, e.g., the typical cross entropy loss $\mathcal{L}(y, q(x; \theta)) = \sum_{i=1}^m -y_i \log q_i$ with q_i be the i -class probability produced by q . And $D_{KL}(p \parallel q) = \mathbb{E}_p[\log(p/q)]$. Furthermore, $\beta \in [0, 1]$ is the distilling weight that balances the empirical loss and KD loss.

¹<https://github.com/facebookresearch/AttentiveNAS>

One could also apply a temperature T to soften (or sharpen) the outputs the teacher model and the student model in KD. More precisely, given an input x , we assume $z_i^p(x)$ and $z_i^q(x)$ the logit for the i -th class produced by p and q , respectively. Then the corresponding predictions of p and q after temperature scaling are as follows,

$$p_i(x; T) = \text{softmax}(z_i^p; T), \quad q_i(x; T) = \text{softmax}(z_i^q; T),$$

with $\text{softmax}(z_i; T) = \exp(z_i/T) / \sum_i \exp(z_i/T)$. In this way, the previous KD objective (7) is now adapted to the following,

$$\begin{aligned} \mathcal{L}(\theta; T) &= (1 - \beta)\mathcal{L}_{\text{ERM}}(\theta) + \beta T^2 \mathcal{L}_{\text{KD}}(\theta; T), \quad \text{with} \\ \mathcal{L}_{\text{KD}}(\theta; T) &= \mathbb{E}_x \left[D_{\text{KL}}(p(x; T) \parallel q(x; T, \theta)) \right]. \end{aligned} \quad (8)$$

Here T^2 is introduced to ensure the gradients from the KD loss is at the same scale w.r.t the gradients from the empirical loss, see (e.g., Hinton et al., 2015). We set $\beta = 0.9$ as default.

D. Related work

Neural architecture search (NAS) NAS offer a powerful tool to automate the design of neural architectures for challenging machine learning tasks. Early NAS solutions usually build upon black-box optimization, e.g. reinforcement learning (e.g., Zoph & Le, 2017), Bayesian optimisation (e.g., Kandasamy et al., 2018), evolutionary algorithms (e.g., Real et al., 2019). These methods find good networks but are extremely computationally expensive in practice. More recent NAS approaches have adopted weight-sharing (Pham et al., 2018) to improve search efficiency. Weight-sharing based approaches often frame NAS as a constrained optimization and solve with continuous relaxation (e.g., Liu et al., 2019; Cai et al., 2019b). However, these methods require to run NAS for each deployment consideration, e.g. a specific latency constraint for a particular mobile device, the total search cost grows linearly with the number of deployment considerations (Cai et al., 2019a). To further alleviate the aforementioned limitations, one-shot supernet-based NAS (e.g., Cai et al., 2019a; Yu et al., 2020; Wang et al., 2020a) proposes to first jointly train all candidate sub-networks specified in the weight-sharing graph such that all sub-networks reach good performance at the end of training; then one can apply typical search algorithms, e.g., genetic search, to find a set of Pareto optimal networks for various deployment scenarios. Overall, one-shot supernet-based methods provide a highly flexible and efficient NAS framework, yielding state-of-the-art empirical NAS performance on various challenging applications (e.g., Cai et al., 2019a; Wang et al., 2020b).

Knowledge Distillation Our knowledge distillation works by forcing the student model to mimic the predictions of the teacher model. As shown in the literature, the feature activations of intermediate layers of the teacher model can also be used as knowledge to supervise the training of the student model, notable examples include (Romero et al., 2014; Huang & Wang, 2017; Ahn et al., 2019; Jang et al., 2019; Passalis & Tefas, 2018; Li et al., 2019, e.g.). Furthermore, correlations between different training examples (e.g. similarity) learned by the teacher model also provide rich information, which could be distilled to the student model (Park et al., 2019; Yim et al., 2017). However, in our work, our KD involves training a large amount of sub-networks (student models) with different architecture configurations, e.g., different network depth, channel width, etc. It is less clear on how to define a good matching in the latent feature space between the teacher supernet and student sub-networks in a consistent way. While our method offers a simple distillation mechanism that is easy to use in practice and in the meantime, leads to significant empirical improvements.

E. Additional results on ablation studies

Following the settings in section 4.2, we provide further analyses on the performance of sub-networks learned under different α and β settings.

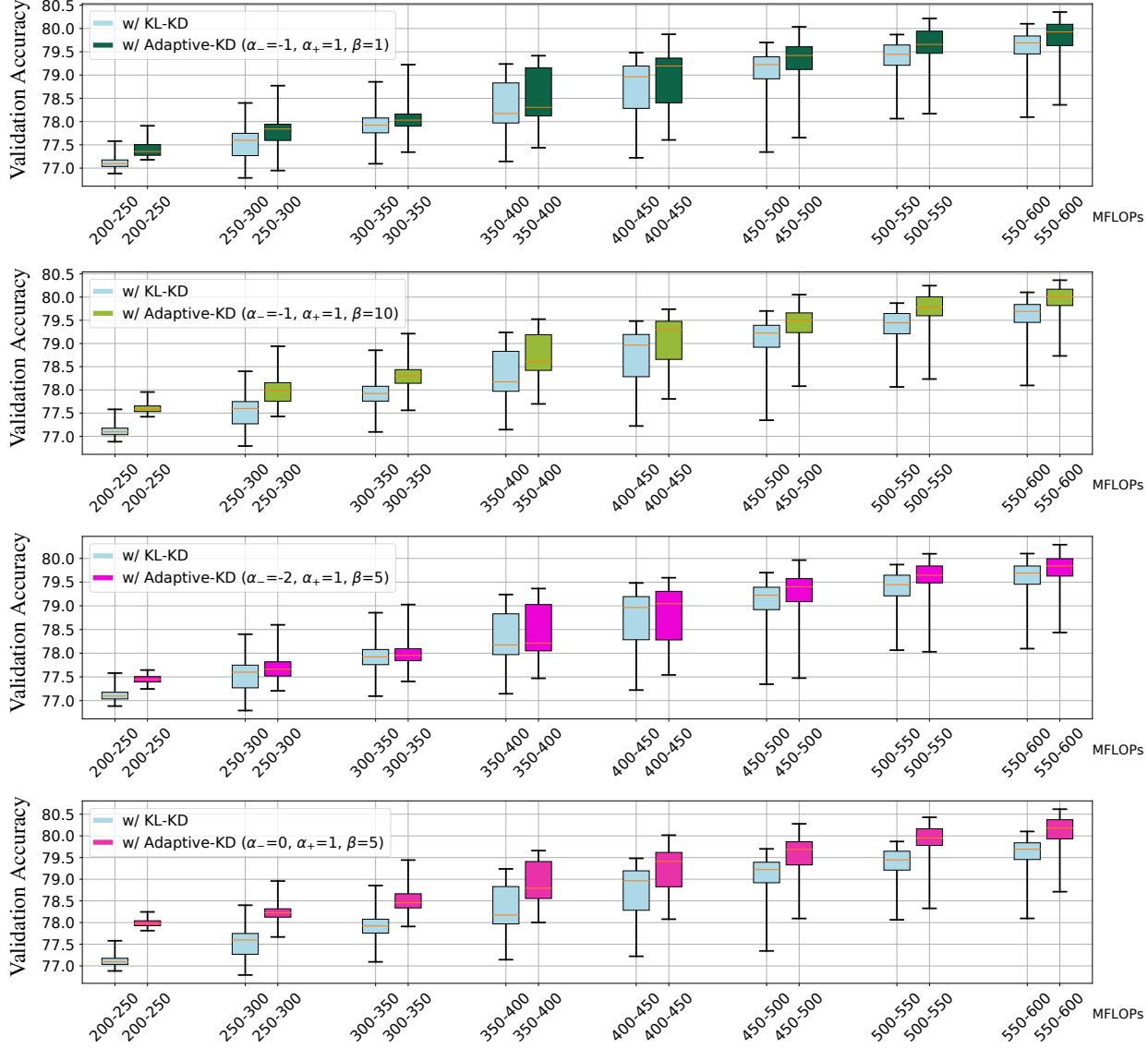


Figure 9. Additional results on ablation studies. Each box plot shows the performance of sampled sub-networks within each FLOPs regime. From bottom to top, each horizontal bar represents the minimum accuracy, the first quartile, the median, the third quartile and the maximum accuracy, respectively.

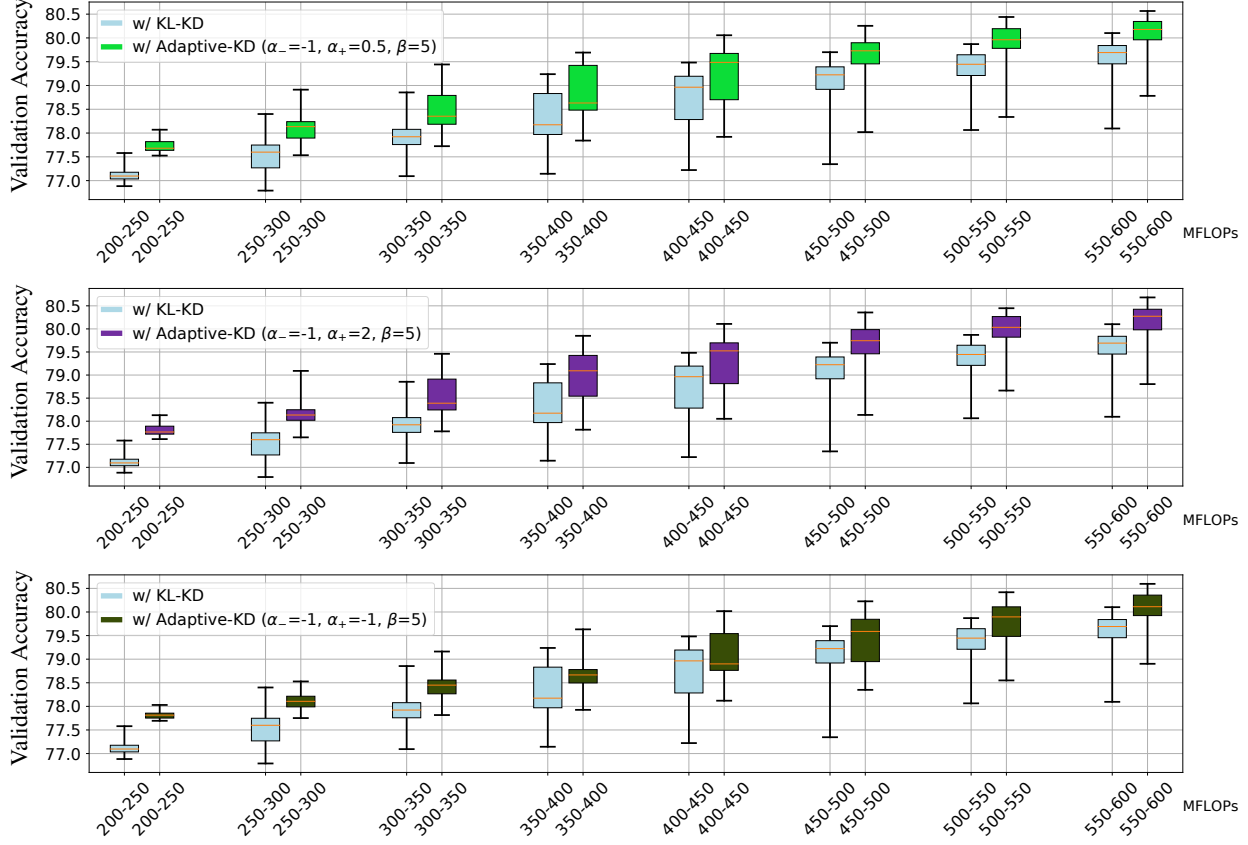


Figure 10. Additional results on ablation studies. Each box plot shows the performance of sampled sub-networks within each FLOPs regime. From bottom to top, each horizontal bar represents the minimum accuracy, the first quartile, the median, the third quartile and the maximum accuracy, respectively.